Temperature-induced droplet coalescence in microchannels

Xu, Bin; Nguyen, Nam-Trung; Wong, Teck Neng

2012

Xu, B., Nguyen, N. T, & Wong, T. N. (2012). Temperature-induced droplet coalescence in microchannels. Biomicrofluidics, 6(1).

https://hdl.handle.net/10356/94430

https://doi.org/10.1063/1.3630124

AIP | Biomicrofluidics

Temperature-induced droplet coalescence in microchannels

Bin Xu, Nam-Trung Nguyen, and Teck Neng Wong

Citation: Biomicrofluidics **6**, 012811 (2012); doi: 10.1063/1.3630124
View online: http://dx.doi.org/10.1063/1.3630124
View Table of Contents: http://bmf.aip.org/resource/1/BIOMGB/v6/i1
Published by the American Institute of Physics.

Temperature-induced droplet coalescence in microchannels

Bin Xu, Nam-Trung Nguyen,[a] and Teck Neng Wong
School of Mechanical and Aerospace, Nanyang Technological University, 50 Nanyang Avenue, Singapore 639798

(Received 12 May 2011; accepted 3 August 2011; published online 15 March 2012)

This paper reports a technique for temperature-induced merging of droplets in a microchannel. The multiphase system consists of water droplet and oil as the dispersed phase and the carrying continuous phase. A resistive heater provides heating in a rectangular merging chamber. The temperature of the chamber is controlled by the voltage applied to the heater. The merging process of two neighboring droplets was investigated with different applied voltage, flow rate ratio between water and oil and total flowrate. Merging is found to be effective at high flow rate ratio, high temperature, and low total flowrate. The presented technique could be used for merging and mixing in droplet-based lab-on-a-chip platforms © *2012 American Institute of Physics*. [doi:10.1063/1.3630124]

I. INTRODUCTION

In recent years, droplet-based microfluidics has been emerged as an alternative for continuous-flow microfluidics. Droplet-based microfluidics has advantages such as fast mixing, short residence time, and low cross contamination[1,2] as compared with single-phase based microfluidics. This new technology has been used in various applications such as microreactor,[2] on-chip polymerase chain reaction (Ref. 3), and protein crystallizations.[4] Mixing of fluids in a droplet requires merging droplets that initially are separated. Droplet coalescence can be achieved by different schemes. Olbricht and Kung realized coalescence utilizing the differences in velocity and size of the droplets.[5] However, coalescence of droplet with the same size and the same velocity is difficult.

In order to achieve complete mixing within a droplet, numerous droplet coalescence techniques have been developed, which can be categorized as passive and active techniques. Passive techniques utilize structure of microchannel to trap droplet in a microchannel. With the help of the structures, the trapped droplet will wait for the subsequent droplet. Two neighboring droplets have a chance to get close to each other due to the drainage of the continuous phase in the fluid resistance element. Kohler *et al.*[6,7] proposed a locally enlarged diameter of fluid channel and a local asymmetry in the cross-section shape to realize droplet coalescence. Tan *et al.*[8,9] developed a trapping method that employs a rectangular expansion, a taped expansion and a flow rectifying structure. Hung *et al.*[10] developed a multifunctional and highly efficient microfluidic device to achieve droplet coalescence. This device consists of three inlets, a double T-junction and a tapered merging chamber. Niu *et al.*[11] employed pillars in the microchannel to initiate droplet coalescence. Active droplet coalescence technique employs energy generated by an external field to realize droplet coalescence. Examples are the droplet coalescence using electro-coalescence,[12–17] dielectrophoresis actuated droplet coalescence[18–20] and pneumatically actuated droplet coalescence.[21]

Most of these previous concepts for droplet coalescence were based on electrostatic forces that require relatively high voltages, which may be harmful for biological applications. Temperature is a parameter that can be more easily controlled using integrated heaters and temperature

[a]Author to whom correspondence should be addressed. Electronic mail: mntnguyen@ntu.edu.sg.

sensors.[22] Baroud *et al.* [23–25] employed a focused laser to enable droplet coalescence. This technique requires extensive setup for the generation of focused laser. In this paper, we report a technique for temperature-induced coalescence of droplets in a microchannel. Experiments were carried out to investigate the effect of applied voltage and consequently of temperature, the flowrate ratio and the total flowrate. The combination of thermocapillary force, lower viscosity, and lower interfacial tension allows controlled coalescence of two droplets.

II. TEMPERATURE-INDUCED DROPLET COALESCENCE CONCEPT

To merge two droplets in a microchannel, the immiscible continuous phase separating them needs to be removed. If the two droplets are positioned in close contact, a thin liquid bridge forms between them due to molecular attraction.[8] The high-curvature meniscus formed around the bridge creates an imbalance of the surface tension leading to coalescence of the two droplets in a short time.[26] The key issue for successful merging of two droplets is to bring them into close contact. In our work, the channel is expanded at the place of merging to slow down the droplets and shorten their distance. The expansion is called the merging chamber. A lower viscosity and lower interfacial tension at high temperature would further slow down the velocity and accelerate the coalescence of the droplets. A heater integrated into the merging chamber is employed to induce the needed temperature.

III. EXPERIMENT

A. Design and fabrication of microfluidic devices

Figures 1(a) and 1(b) show the schematic layout of the microfluidic device used in our experiments. Droplets generated at the flow-focusing junction are directed to merging chamber. The microchannel has a rectangular cross section of 200×400 μm. The square chamber has a width of 1000 μm. The heating wire is inserted into the slot in the top part, Figure 1(c).

The structure of the microchannel was cut by using a CO_2.laer cutting system (Universal Laser Systems Inc., laser power of 25 W and a maximum beam speed of about 640 mm/s). The width of the microchannel was determined by the width of the drawn lines, where the depth of the microchannel was controlled by the power and the speed of the laser beam. The fabrication is based on the lamination thermal bonding technique.[27] In this method, two polymethylmethacrylate (PMMA) plates (60 mm $\times$ 25 mm) were bonded together to form a closed microfluidic channel with inlet and outlet holes. The two PMMA parts are thermally bonded using a hot press (CARVER manual press 4386). The temperature of the hot plate was kept at 80 °C for 20 min, subsequently raised to 170 °C and then kept for another 20 min. Finally, the device was allowed to cool down to room temperature.

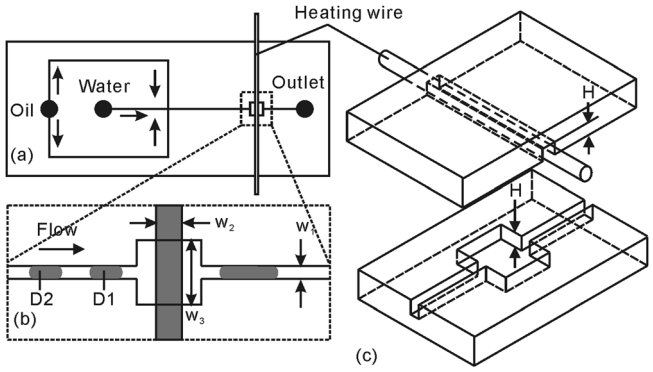

FIG. 1. (a) Schematic illustration of the microfluidic device for droplet merging. Droplets are formed at the first junction (droplet formation junction) and then merge at the second junction (droplet coalescence junction), (b) Enlarged schematics of the merging chamber ($W_2 = 400\,\mu$m,$W_3 = 1000\,\mu$m), and (c) Exploded view of the top and bottom parts to form the merging chamber ($W_1 = 200\,\mu$m,$H = 400\,\mu$m).

B. Materials

De-ionized (DI) water and mineral oil (Sigma M5904, St. Louis) were used as the dispersed phase for the droplet and the continuous carrying phase, respectively. Fluorescent dye (Fluorescein disodium salt $C_{20}H_{10}Na_2O_5$) was added into DI-water for the later visualization of the droplets. Non-ionic surfactant Span 80 (Sigma S6760) 2% by weight was added into the mineral oil to assist and stabilize the formation process of droplets. The liquids were delivered by a syringe pump (KDS230, KD Scientific Inc., 0.2-500 μl/h, accuracy of 0.5%). A DC power supply (GW, Model GPC-30300) provides the voltage for the heating wire (Newport NIC80, 80% Ni, 20% Cr, 0.2 mm diameter, and 80 Ω/m). An inverted microscope (Nikon, ECLIPSE TE2000-S) with a set of epi-fluorescent attachments and a coupled charge device (CCD) camera (Sony ICX 084, 1324×1024 pixels, 16 bits grayscale) was used for recording the fluorescence images.

C. Experimental setup

A schematic experimental setup is shown in Figure 2. The setup consists of four main components: an illumination system, an optical system, a CCD camera, and a personal computer (PC) based control system. A mercury lamp with the wave length of 532 nm was employed as the illumination source for the fluorescence imaging setup.

The Nikon inverted microscope (Model ECLIPSE TE2000-S) with a set of epi-fluorescent attachments was used as the optical system. Excitation filter, dichroic mirror, and emission filter constitute the filter cube. Emission filters were used in the measurements to select the specific emission wavelength of the sample and to remove the traces of excitation light. An interline transfer CCD camera (Sony ICX 084) was used for recording the images. The resolution of the camera is 1324×1024 pixels with 16 bits grayscale.

In the experiment, a soft Cole Parmer tube (Vernon Hills, Illinois 60061) was employed to connect the syringe and the microfluidic device. The DI-water and the mineral oil in the syringes were introduced into the inlet A and B, respectively, by using the syringe pumps. The DC power supply was used to provide an electric field to the nickel chrome wire.

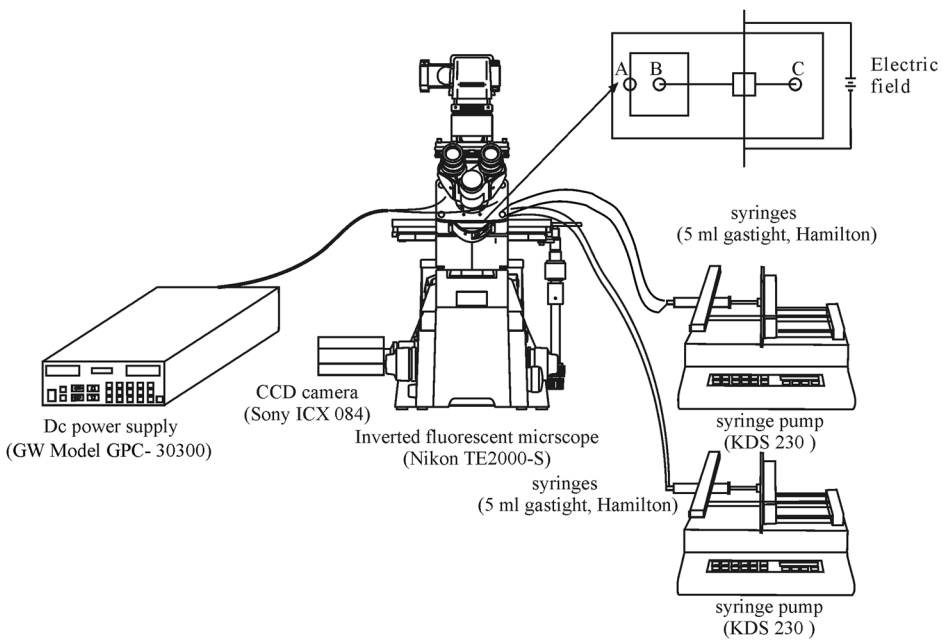

FIG. 2. Schematic illustration of the experimental setup.

IV. RESULTS AND DISCUSSIONS

The three parameters investigated are the applied voltage, the flowrate ratio between the dispersed phase (DI-water) and the continuous phase (mineral oil) $\beta = Q_{water}/Q_{oil}$, and the total flowrate. A calibrated K-type fine wire gauge thermocouple was used to measure the temperature of the merging chamber filled with mineral oil. Figure 3 shows a second-order relationship between the temperature and the applied voltage, because the temperature is proportional to the heating power which in turn is a square function of the applied voltage. Since inserting the thermocouple into the merging chamber during the experiment would affect the coalescence process and block the view of the camera, the temperature values in Figure 3 are used to estimate the actual temperature in the chamber under flow conditions. The later results are discussed in term of heating voltage and not temperature, which cannot be monitored during the experiment.

A. Effect of applied voltage

Figure 4 compares the behavior of two droplets in the merging chamber with and without heating. Without heating (Figure 4(a)), the first droplet (D1) enters the chamber at t = 0 s. In the chamber, droplet D1 decelerates due to the lower flow velocity in the extended chamber. At t = 4 s, droplet D1 approaches the exit of the chamber, while the second droplet (D2) just enters it. When D2 was completely inside the chamber, as D1 was already left. The two droplets have no opportunity to come in close contact and cannot be merged because of the oil phase separating them. Figure 4(b) shows the behavior of two droplets formed under the same condition of the case depicted in Figure 4(a). However, a voltage of 1 V is applied to the heater. After 2 s, droplet D1 is completely inside the chamber. At t = 4 s, instead of moving forward D1 remains trapped at the exit and waits for the subsequent droplet D2 to enter the chamber. When D1 and D2 come to a close contact, D2 pushes D1 to initiate a slight forward motion (t = 6 s). The two droplets subsequently merge at t = 8 s. After turning off the applied voltage, it takes about 3 s to cool down to room temperature.

The physics behind the observed coalescence can be explained by a two-step process of competition between thermocapillary force and pressure as well as hydrodynamic drag force. The first step occurs at the entrance of the merging chamber, while the second step happens at the exit. Before entering the chamber, the droplets move at a constant velocity within the continuous phase (mineral oil). Once a droplet is inside the merging chamber, the average flow velocity of droplet and oil will decreases due to the expansion. At a higher temperature induced by the wire heater, the viscosity of the continuous phase decreases. As a result, the oil in the

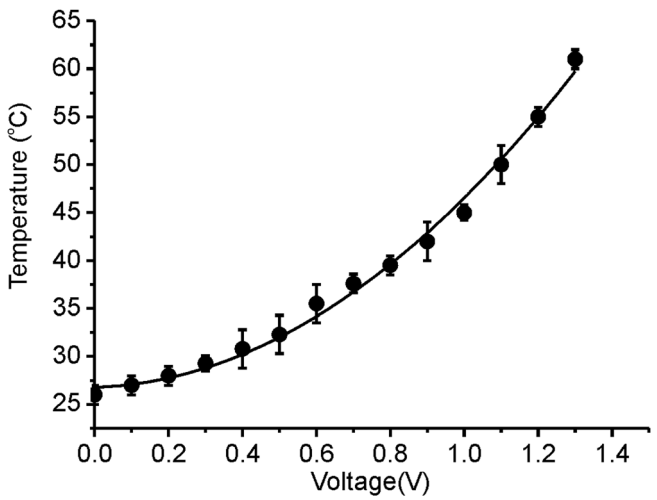

FIG. 3. Temperature of the merging chamber as a function of applied voltage.

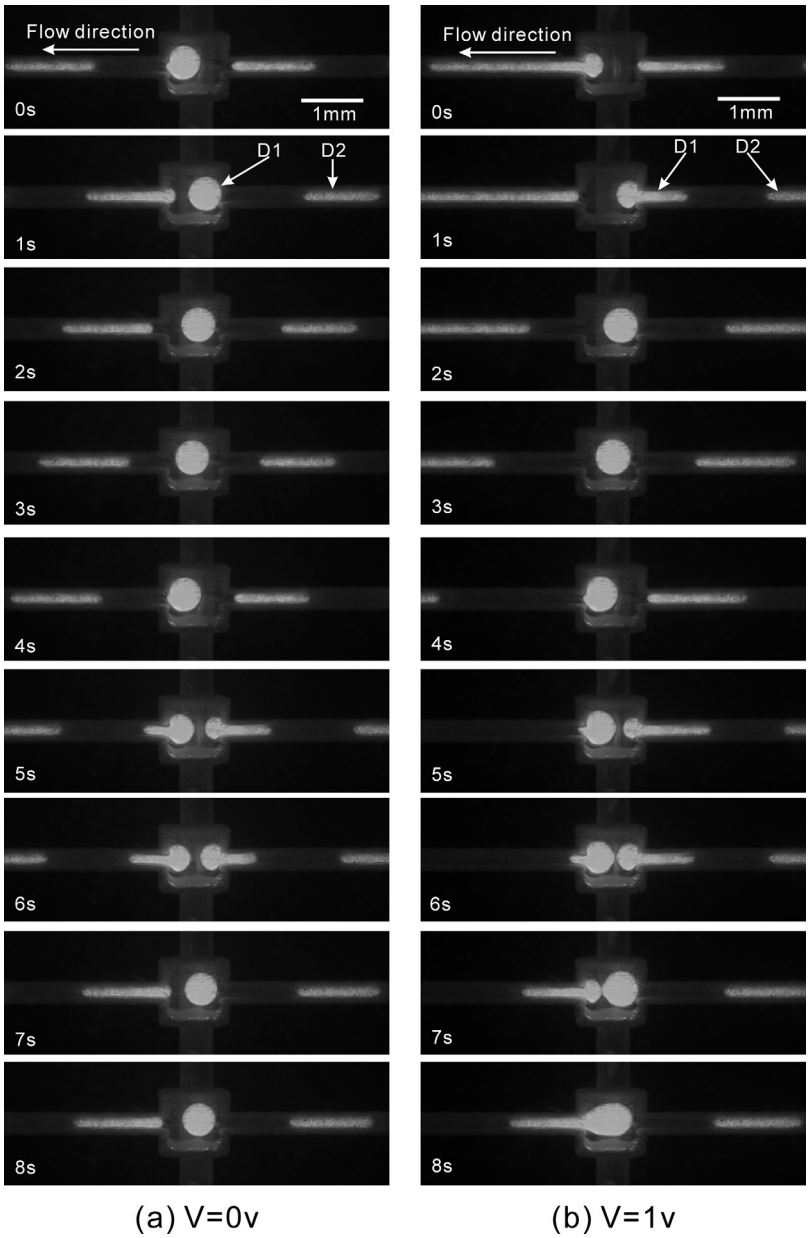

FIG. 4. Behavior of two droplets in the merging chamber ($Q_{water} = 100\,\mu$l/h,$Q_{oil} = 200\,\mu$l/h): (a) without heat (V = 0 v); (b) with heat (V = 1 v).

chamber can flow faster to escape the chamber allowing the droplet to stay longer in the chamber. Moreover, a gradient of surface tension between the head and the tail of the droplet emerges due to the distributed temperature around the heater. The hot head of the droplet has a smaller surface tension than the cold tail. Thermocapillary force pushes the droplet to move forward. However, when the head of droplet reaches the exit of the chamber, the head is colder than the tail. Thermocapillary force counters the hydrodynamic drag force and decelerates the droplet. The balance between these two forces allows the first droplet to remain at the exit of the merging chamber waiting for the next droplet. With the second droplet D2 inside the chamber, thermocapillary forces push D1 backward and D2 forward initiating merging. As the droplets, D1 and D2 come into close contact after the drainage of the oil between them, a singularity occurs at the joint of the two droplets. As time goes by, a connecting bridge forms between the two droplets. Evidently, the meniscus around the bridge is a region of very high

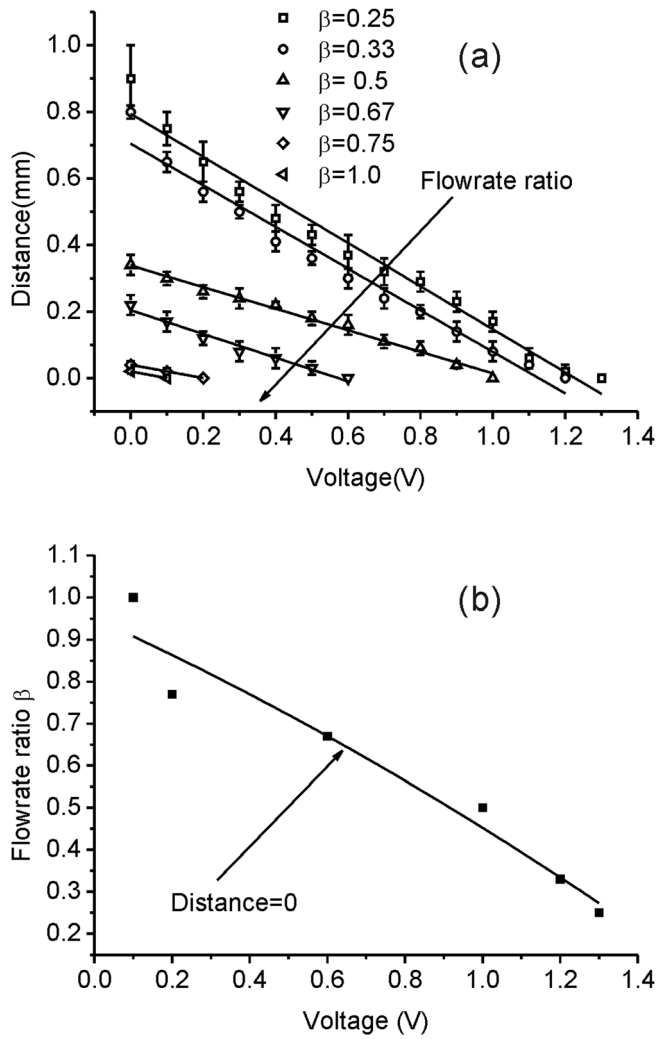

FIG. 5. Droplet behavior in the merging chamber: (a) Distance between two neighboring droplets at different flowrate ratio and heating voltage; and (b) Relationship between the flowrate ratio and the threshold voltage required for merging.

curvature, which increases the radius of the tiny bridge. The breakage of this bridge results from a thermocapillary force. Subsequently, the merged droplet is big enough to block the exit of the chamber, increasing the pressure inside the chamber. As a result, despite of the thermocapillary force, the merged droplet can be released from the chamber and makes place for the next two droplets.

B. Effect of flowrate ratio

The behavior of the two droplets in the merging chamber was subsequently investigated for different combination of flowrate ratios. Figure 5(a) shows the variation of the gap between the two droplets in the merging chamber as a function of the applied voltage. The solid line for each is a liner fitting function. A gap of zero means that the two droplets are able to coalescence. At a given flowrate ratio, the distance between two neighboring droplets decreases with increasing applied voltage. At a given applied voltage, the gap decrease as the flowrate ratio increases. At a higher flowrate ratio, the water droplets are larger than the oil separating them. At a threshold voltage, the gap is closed and the droplets are merged. The relationship between the flowrate ratio and the corresponding threshold voltage is shown in Figure 5(b). A large flowrate ratio results in a small gap and only requires a low voltage to close it.

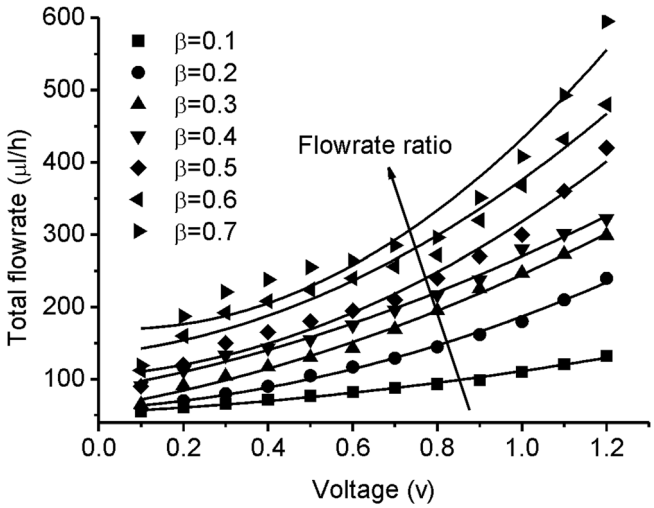

FIG. 6. Droplet behavior in the merging chamber: Relationship between the total flowrate and the threshold voltage required for merging at different flowrate ratio.

C. Effect of total flowrate

The behavior of two droplets in the merging chamber was inherently studied for different total flowrates. Figure 6 shows the relationship between the total flowrate and the corresponding threshold voltage at different flowrate ratios. The solid line for each is a second-order fitting function. At a given flowrate ratio, the threshold voltage increases as the total flowrate increases. At a low total flowrate, the water droplets and oil move at a relatively low velocity, which requires a low voltage to merge it.

V. CONCLUSIONS

We report a concept to merge two identical droplets in a microchannel. The droplets are trapped and manipulated in a rectangular merging chamber. The merging process is controlled by the voltage applied to a wire heater in the merging chamber. This method is effective for high flowrate ratio, low total flowrate, and high temperature. The high flowrate ratio makes sure that the droplets are in reasonable close contact and can remain in the chamber at the same time for merging. The low total flowrate ensures the low velocity of droplets in the chamber. The high temperature reduces the viscosities and the interfacial tension, and at the same time increases the thermocapillary forces. The concept presented in this paper could potentially be used for merging and mixing in droplet-based lab-on-a-chip replacing previous continuous-flow counter parts.[28] One of the most important applications for droplet coalescence in such a device is the mixing of reagents. Mixing can be achieved in the merging chamber when droplets containing different reagents are mixed.

[1]K. Handique and M. A. Burns, J. Micromech. Microeng. **11**(5), 548 (2001).
[2]H. Song, D. L. Chen, and R. F. Ismagilov, Angew. Chem., Int. Ed. **45**(44), 7336 (2006).
[3]Z. Guttenberg, H. Müller, H. Habermüller, A. Geisbauer, J. Pipper, J. Felbel, M. Kielpinski, J. Scriba, and A. Wixforth, Lab Chip **5**(3), 308 (2005).
[4]B. Zheng, L. S. Roach, and R. F. Ismagilov, J. Am. Chem. Soc. **125**(37), 11170 (2003).
[5]W. L. Olbricht and D. M. Kung, J. Colloid Interface Sci. **120**(1), 229 (1987).
[6]J. M. Köhler, T. Henkel, A. Grodrian, T. Kirner, M. Roth, K. Martin, and J. Metze, Chem. Eng. J. **101**(1-3), 201 (2004).
[7]V. Chokkalingam , B. Weidenhof, M. Krämer, W. F. Maier, S. Herminghaus, and R. Seemann, Lab Chip **10**(13), 1700 (2010).
[8]Y. C. Tan, J. S. Fisher, A. I. Lee, V. Cristini, and A. P. Lee, Lab Chip **4**(4), 292 (2004).
[9]N. Bremond, A. R. Thiam, and J. Bibette, Phys. Rev. Lett. **100**(2), 024501 (2008).
[10]L. H. Hung, K. M. Choi, W. Y. Tseng, Y. C. Tan, K. J. Shea, and A. P. Lee, Lab Chip **6**(2), 174 (2006).
[11]X. Niu, S. Gulati, J. B. Edel, and A. J. Demello, Lab Chip **8**(11), 1837 (2008).
[12]M. Chabert, K. D. Dorfman, and J. L. Viovy, Electrophoresis, **26**(19), 3706 (2005).

[13]D. R. Link, E. Grasland-Mongrain, A. Duri, F. Sarrazin, Z. Cheng, G. Cristobal, M. Marquez, and D. A. Weitz, Angew. Chem., Int. Ed., **45**(16), 2556 (2006).
[14]F. Sarrazin, L. Prat, N. Di Miceli, G. Cristobal, D. R. Link, and D. A. Weitz, Chem. Eng. Sci. **62**(4), 1042 (2007).
[15]M. Zagnoni, G. Le Lain, and J. M. Cooper, Langmuir **26**(18), 14443 (2010).
[16]X. Niu, F. Gielen, A. J. DeMello, and J. B. Edel, Anal. Chem. **81**(17), 7321 (2009).
[17]W. Wang, C. Yang, and C. M. Li, Small **5**(10), 1149 (2009).
[18]J. A. Schwartz, J. V. Vykoukal, and P. R. C. Gascoyne, Lab Chip **4**(1), 11 (2004).
[19]P. Singh and N. Aubry, Electrophoresis **28**(4), 644 (2007).
[20]W. Wang, C. Yang, and C. M. Li, Lab Chip **9**(11), 1504 (2009).
[21]B. C. Lin and Y. C. Su, J. Micromech. Microeng. **18**(11), 115005 (2008).
[22]N. T. Nguyen and X. Huang, Jpn. J. Appl. Phys., Part 1 **44**(2), 1139 (2005).
[23]C. N. Baroud, M. Robert De Saint Vincent, and J. P. Delville, Lab Chip **7**(8), 1029 (2007).
[24]R. M. Lorenz, J. S. Edgar, G. D. M. Jeffries, Y. Zhao, D. McGloin, and D. T. Chiu, Anal. Chem. **79**(1), 224 (2007).
[25]I. R. Perch-Nielsen, P. J. Rodrigo, C. A. Alonzo, and J. Glückstad, Opt. Express **14**(25), 12199 (2006).
[26]J. Eggers, J. R. Lister, and H. A. Stone, J. Fluid Mech. **401**, 293 (1999).
[27]Y. Sun, Y. C. Kwok, and N. T. Nguyen, J. Micromech. Microeng. **16**(8), 1681 (2006).
[28]H. Y. Tan, W. K. Loke, Y. T. Tan, and N. T. Nguyen, Lab Chip **8**(6), 885 (2008).